Photochemistry of Biphenyl Occluded within X Faujasite Type Zeolites

Isabelle Gener,† Guy Buntinx, Alain Moissette, and Claude Brémard*

Laboratoire de Spectrochimie Infrarouge et Raman UMR-CNRS 8516, Centre d' Etudes et de Recherches Lasers et Applications, Bât. C5 Université des Sciences et Technologies de Lille I, 59655 Villeneuve d'Ascq Cedex, France

Received: February 19, 2002; In Final Form: July 12, 2002

The UV laser flash photolysis (248 nm, 10 ns) of biphenyl (BP) occluded in void space of aluminum rich faujasitic X zeolites $Na_n(AlO_2)_n(SiO_2)_{192-n}$ with $n = 85, 96$ has been investigated by diffuse reflectance transient UV−visible absorption (DRTUV) and time-resolved resonance Raman (TR^3) measurements on the nano- and microsecond time scales. TR^3 measurements were carried out using an 8 ns probe pulse at 370 nm. Delays between pump and probe pulses (50 ns to 100 μs) provide evidence of triplet state $BP(T_1)$, radical cation $BP^{\bullet+}$, and radical anion $BP^{\bullet-}$ with planar quinoidal structures. Self-modeling mixture analysis (SIMPLISMA) of DRTUV data sets resolved pure absorption spectra of $BP(T_1)$, $BP^{\bullet+}$, $BP^{\bullet-}$, and trapped electron as Na_4^{3+}. Data processing determines also the decays of the corresponding concentrations between 0.5 and 340 μs for loading values corresponding to 1, 2, 4, and 8 BP per unit cell. All the decays of specific concentration were found to fit a model of dispersed heterogeneous kinetics. At lower laser fluence, $BP(T_1)$ was found to be the major transient species for all the loading values. Lifetime mean values of $BP(T_1)$ were found to be 40 and 110 μs at low and high loading, respectively. Photoionization was found to be dominant at higher pump laser fluence. At low loading, Na_4^{3+} cluster and $BP^{\bullet+}$ are produced in high yield with relatively different lifetimes, 10 μs and ∼500 μs, respectively. The recombination process includes probably supplementary electron transfers with the zeolite framework. At high loading, $BP^{\bullet-}$ (20 μs) concomitantly forms $BP^{\bullet+}$ (12 μs) as a result of photoejected electron capture by $BP(S_0)$. The most important role of porous solids with large pores such as X faujasite with respect to photophysical and photochemical BP behaviors in solution appears to be the efficient trapping of photoejected electron in the solid network.

Introduction

Biphenyl and its chlorine- and bromine-substitutive derivatives have been used in a variety of industrial and agrochemical applications such as insecticide, organic diluents, flame retardants, or plasticizers. These man-made pollutants are insoluble in water and tend to accumulate in fats or oils or on the surface of inorganic solids of the environment. The sunlight initiates reactions that lead to transformation or decomposition of organic contaminants into more or less toxic products.

The photochemical and photophysical behaviors of biphenyl and, to a lesser extent, chlorobiphenyls are well-known in solution.[1−4] Less attention has been paid to these behaviors on the inorganic surfaces including TiO_2, SiO_2, Al_2O_3, clays, or zeolites.[5−8] The ever-increasing interest in photochemistry in heterogeneous media has prompted investigations of polyaromatics occluded in zeolites.[9,10] Zeolites are crystalline microporous aluminosilicates that contain organized openings and void spaces of molecular dimensions. Zeolites are very convenient polar hosts that are capable of modifying photochemical properties of sorbates.[11−13] Transient absorption studies of several aromatic molecules sorbed in cavities of zeolites have been carried out and several unique aspects of photophysics and photochemistry of these aromatic molecules have been revealed.[6] There still remain some uncertainties about photoionization of biphenyl concerning particularly the fate of photoejected electrons from guests to electron scavengers. Detailed kinetic analysis of decays of transient species is missing.

In a recent work, we have published results about sorption sites and dynamics of biphenyl (BP) in the ground state within the void space of X type zeolites.[14] Zeolite X used in industry is the synthetic analogue of the mineral faujasite. These zeolites have the following chemical composition $Na_n(AlO_2)_n(SiO_2)_{192-n}$, where n is between 77 and 96, and are abbreviated hereafter Na_nFAU. In the present article, we have studied spectroscopy, structure, and lifetime of transient species generated through laser photolysis of biphenyl occluded in the porous void of Na_n-FAU. These photochemical and photophysical properties were explored as functions of biphenyl loading and laser fluence. The transient species identification and corresponding lifetimes were deduced from diffuse reflectance transient UV−visible absorption spectroscopy (DRTUV) and time-resolved resonance Raman scattering (TR^3) investigations on the nano/microsecond time scale thanks to the SIMPLISMA self-modeling mixture analysis approach. We have initiated the present work to gain a comprehensive understanding of the general dynamic picture of transient species generated by a laser pulse in zeolites with medium large cavities, high aluminum content, and numerous Na^+ extraframework cations.

Experimental Section

Materials. Na_{85}FAU (Na_{85}X) and Na_{96}FAU (Na_{96}X) zeolites were obtained from CeCa. Biphenyl (BP) was purchased from

* To whom correspondence should be addressed: Fax: +33(0)-320434965. E-mail bremard@univ-lille1.fr.

† Present address: Laboratoire de Catalyse en Chimie Organique, UMR-CNRS 8503, Université de Poitiers, 40 avenue du recteur Pineau, 86022 Poitiers, France.

10.1021/jp020454d CCC: $22.00
Published on Web 09/12/2002

Merck-Schuchardt and was bisublimed. Weighted amounts (~1.4 g) of powdered hydrated zeolite Na_nFAU ($n = 85, 96$) were introduced into an evacuable heatable silica cell. The sample was dried under vacuum (10^{-3} Pa) and heated stepwise to 773 K under air. Oxygen was then admitted into the cell for 6 h at 773 K. The thermal treatment completely removed occluded water molecules and organic impurities.[15] The crystallinity of the samples was checked by XRD and was not reduced by calcination treatment. Then, the sample was held under vacuum and cooled to room temperature under dry argon. Weighted amounts of bisublimated BP, corresponding to 1, 2, 4, or 8 BP per unit cell (UC) loadings, were introduced into the cell under dry Ar and the powder mixture was shaken. After 4 weeks at 50 °C, the sample was transferred under dry argon in a quartz glass Suprasil cuvette.

Instrumentation. Elemental analyses (C, H, Al, Si, Na, O) of the bare and loaded zeolites were obtained from the Service Central d'Analyse du Centre National de la Recherche Scientifique (Vernaison, France).

DRUV spectra were recorded at room temperature between 200 and 850 nm using a Cary 3 spectrometer equipped with integrating spheres. The corresponding bare zeolite was used as reference. A Bruker IFS 88 FT-Raman spectrometer with Cw Nd:YAG laser at 1064 nm as the excitation source was used; 50−200 mW laser power was used. Spectra (3500−150 cm^{-1}) were recorded with 2 cm^{-1} resolution using 400 scans. The Opus Bruker software was used for spectral acquisition, data treatment, and plotting.

The experimental setup of nanosecond diffuse reflectance laser photolysis, applicable to the detection of transient species (DRTUV) in optically inhomogeneous and light-scattering media was similar to that previously described.[16] It included an excimer laser as the pump source (248 nm, 0.15−1.5 mJ, 10 ns, 0.3 Hz) and a xenon arc lamp as the probe source. Kinetics at different wavelengths were accumulated over 10 laser pulses. The DRTUV data were described by

$$\text{absorption} \qquad D(\lambda,t) = [1 - R(\lambda,t)/R_0(\lambda,t)] \tag{1}$$

where R and R_0 denote the intensities of diffused reflected light with and without excitation, respectively. In the case where D absorption is relatively low, it has been shown that the concentration C of the transient will be directly proportional to D. The former function was used to both simulate the spectra and treat the kinetics of the transients.

The nanosecond TR^3 set up has been detailed elsewhere.[2,17]

It used an excimer laser (Questek 2040) as the pump excitation (248 nm, 1 mJ, about 1.5 J/cm^2, 10 ns, 10 Hz), a Nd:Yag + dye laser system (Quantel 581C, and TLD50) as the probe pulse (370 nm, 1.5 mJ, 8 ns, 10 Hz), a gated intensified diode array (20-ns gate) as the detector, and a home-built spectrometer. The spectral resolution and the analyzed field were about 8 and 1600 cm^{-1} respectively, at 370 nm. The probe pulse was delayed with respect to the pump using a homemade generator. For measurements of solid samples a rotating cell was used and rejection of the elastic and inelastic diffused light was made by Notch filters.

Self-Modeling Mixture Analysis. The data processing of DRTUV spectra $D(\lambda,t)$ was carried out using the SIMPLISMA (simple-to-use interactive self-modeling mixture analysis) approach.[18,19] This method was applied to extract pure Raman spectra (P) and the respective concentration (C) from a huge amount of spectral data of mixtures without any prior information. The mathematical principle of SIMPLISMA lies in the presence of a pure or key variable. A key variable (wavelength or wavenumber for absorption spectra) is hypothetically a variable that has an intensity contribution from only one of the mixture components. Such a requirement is not automatically met for each data set under study. When such situations occur, the possibility of resolving data property by using second derivative spectra as an intermediate step has been shown.[20,21] So, once experimental spectra have been twice derived, the sign of the so-called spectra is changed to obtain positive peaks at the same wavenumber where the original spectra had theirs. As a consequence, the operation was referred to inverted second derivative spectra. The so-called spectra still have negative parts, which is very problematic for the pure variable approach that inherently requires positive spectra. Previous works dealing with this problem showed the validity of setting negative values of the transformed spectra to zero. That implies in the present work an almost complete elimination of overlapped absorption bands.

Pure variable intensities can be used as a concentration estimate in the following relation.

$$\mathbf{D} = \mathbf{C}\mathbf{P}^{\mathrm{T}} \tag{2}$$

D represents the original data matrix with spectra in rows; **C** represents the "concentration" matrix, obtained by using the columns of **C** that represent key variables. **P** represents the matrix with the spectra of the pure components in its columns; $\mathbf{P}^{\mathrm{T}}$ represents the transpose of **P**. Typically, **D** exists but **C** and **P** are not known. When the matrices **D** and **C** are known (**C** becomes known through the SIMPLISMA algorithm), **P** can be calculated by standard matrix algebra.

$$\mathbf{P} = \mathbf{D}^{\mathrm{T}}\mathbf{C}(\mathbf{C}^{\mathrm{T}}\mathbf{C})^{-1} \tag{3}$$

In a next step, the contributions are now calculated from **P**, which are basically a projection of the original pure variable intensities in the original data set. This step reduces the noise in the contributions. The equation is

$$\mathbf{C}^* = \mathbf{D}\mathbf{P}(\mathbf{P}^{\mathrm{T}}\mathbf{P})^{-1} \tag{4}$$

where **C*** stands for the projected **C**. Because matrix **C** does not contain concentrations but intensities proportional to concentrations, scaling procedures such as normalization of the resulting spectra in **P** and the associated inverse normalization of **C** are often used to obtain the relative contributions of the components. The data set can be reconstructed as follows:

$$\mathbf{D}^{\text{calculated}} = \mathbf{C}^*\mathbf{P}^{\mathrm{T}} \tag{5}$$

The relative root sum of squares (RRSSQ) coefficient calculates residuals and represents the difference between the reconstructed and the original data. This coefficient can be seen as a standard deviation and was defined previously. The values are between 0 and 1. The algorithm for pure variables in SIMPLISMA is detailed elsewhere.[18,19]

Kinetic Data Processing. Data processing using SIMPLISMA software of the DRTUV spectral set gives the respective contribution of each absorbing transient species as a function of time despite severe spectral overlap. The simplest kinetic analysis of the $C(t)$ decay has been tested in terms of one, two, or three exponentials. They do not accurately reproduce the decays. The concentration functions $C(t)$ were accurately fitted using the Albery function.[22] This Gaussian distribution kinetic model is based on dispersion of the first-order rate constants $k = \bar{k}\exp(\gamma x)$; $\bar{k}$ is the average rate constant and γ is the width of the distribution.

Several attempts were made with other empirical or fractal approaches, but they do not accurately reproduce the decays.[23]

Molecular Modeling. The molecular modeling of the sorption was generated using the program Cerius[2] developed by Molecular Simulation Inc. The details of the calculations are identical to those reported recently.[14]

Results

Sorption of BP in Na_nFAU (n = 85, 96). Weighted amounts of dry BP were added to dehydrated porous material under dry Ar without any solvent. The weighted BP amounts correspond to 1, 2, 4, or 8 BP per unit cell of Na_nFAU ($Na_n(AlO_2)_n(SiO_2)_{192-n}$) with n = 85 and 96. The aluminosilicate framework of X zeolite is built from cubooctahedral sodalite cages linked together via hexagonal prisms in an arrangement that gives rise at their center to "supercages", 12.5 Å in diameter. Each "supercage" is connected to four others through near circular windows (12-membered rings) ca. 8 Å in diameter. The negative charge of the skeleton formed by SiO_4 and AlO_4 tetrahedra is compensated by exchangeable Na^+ cations spread in the cavities.[24,25] Progressively, by sublimation BP molecules pass through the windows of porous void space and migrate relatively slowly in cavities. The sorption goes to completion over several weeks at room temperature. All the spectroscopic and diffraction measurements (see Experimental Section) carried out on equilibrated samples were found to be in accurate agreement with BP occluded in the void space of Na_nFAU.[14] Zeolites were loaded with BP under strict anhydrous conditions and without any solvent.[26] The effects of possible residual water on photolysis were checked by the introduction of calculated amounts of water in dehydrated samples.

Diffuse Reflectance Transient UV−Visible Absorption. BP occluded at low loading (1 BP/UC) in Na_nFAU (n = 85, 96) exhibits intense and broad absorption around 250 nm; this absorption is assigned to the $S_3 \leftarrow S_0$ transition, which is of the $\pi^* \leftarrow \pi$ type by comparison with previous results in solution.[1,2] However, the shape and absorption coefficient were found to be highly dependent on zeolite loading.[14] UV flash photolysis was carried out with the laser line wavelength centered around the broad absorption. The nanosecond laser pump (10 ns, 248 nm) was combined with transient UV−visible absorption spectroscopy in the 300−750 nm wavelength range using the diffuse reflectance technique. DRTUV experiments were carried out for a series of completely equilibrated powdered samples between 0.5 and 340 μs. At short times, a very intense fluorescence is observed, which prevents the recording of absorption spectra below 0.5 μs.

Figures 2−4 show the transient absorption spectra recorded at different delays after the excitation laser pulse for three loading levels. It is clear from examination of Figures 2−4 that spectra series are highly dependent on loading values. In addition, it was found that for corresponding loading values, spectra markedly change with laser fluence (0.2 and 4 mJ.cm^{-2}) whereas they hardly change with the aluminum content of zeolite (n = 85, 96).

At low loading (1 BP/UC), Figure 2, SIMPLISMA analysis[18,19] of the spectral set including all spectra recorded between 0.5 and 340 μs after the laser pulse with fluence between 0.2 and 4 mJ·cm^{-2} permits us to resolve three spectra, Figure 5a,b,d. The spectra in (a) and (b) were straightforwardly attributed to $BP(T_1)$ and $BP^{\bullet+}$ by comparison with the spectra previously obtained in solution.[1,2] The band at 360 nm was assigned to the $T_n \leftarrow T_1$ transition, whereas the bands observed at 375 and 675 nm were assigned to $^*BP^{\bullet+} \leftarrow BP^{\bullet+}$ transitions.[2] The extracted spectrum b exhibits a broad absorption with a maximum at 510 nm assigned to the Na_4^{3+} cluster as a major trapping site. The assignment was based on the previous observation of a similar band on γ or pulsed electron irradiation of dehydrated NaX.[27−29] The electron trapping as the Na_4^{3+} cluster seems immediate in the experimental time scale and

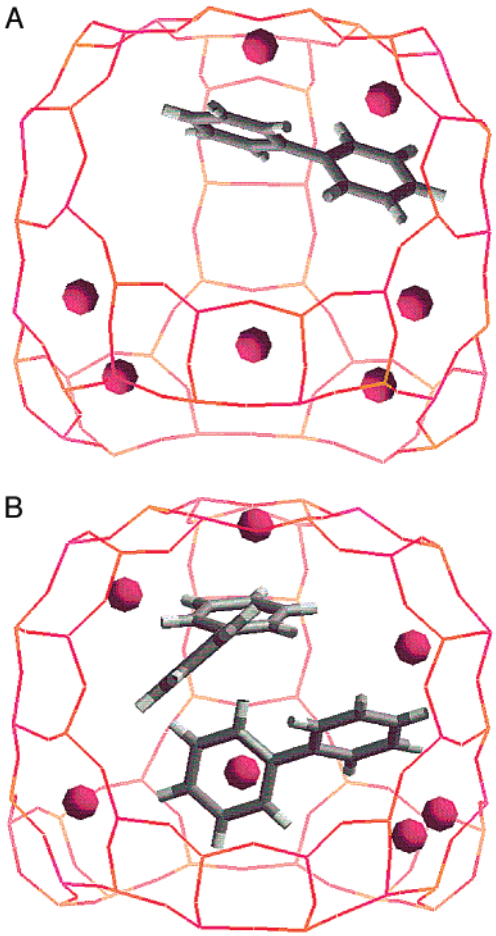

Figure 1. (A) Predicted conformation and sorption site of biphenyl (BP) occluded in a supercage of Na_{96}FAU zeolite at low loading (1BP/Na_{96}FAU). (B) Predicted conformations and sorption sites of 2 BP occluded in a supercage at high loading (8 BP/Na_{96}FAU). The pictures result from energy minimization. The red, yellow, and pink sticks represent the O, Si, and Al atoms of the $(AlO_2)_{96}(SiO_2)_{96}$ framework, respectively. The pink balls represent the Na^+ cations. The white and gray cylinders represent the H and C atoms of BP, respectively.

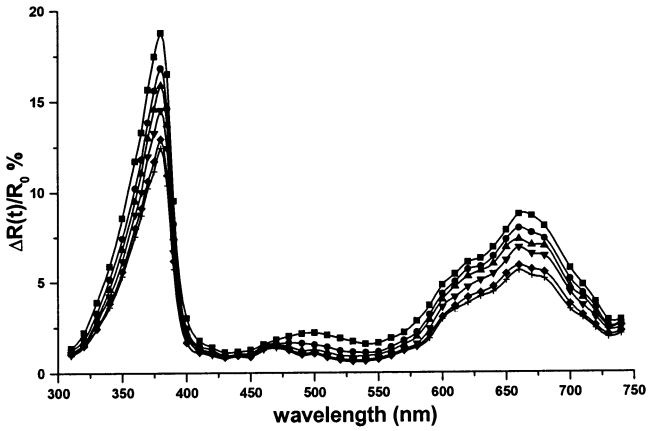

Figure 2. Diffuse reflectance transient UV−visible absorption spectra of photoexcited BP occluded in Na_{85}FAU at 1 BP/UC loading recorded at different delay times 1.5 (■), 5 (●), 10 (▲), 30 (▼), 90 (◆), and 130 (+) μs after laser pump excitation (248 nm, 10 ns, 1.5 mJ·cm^{-2}).

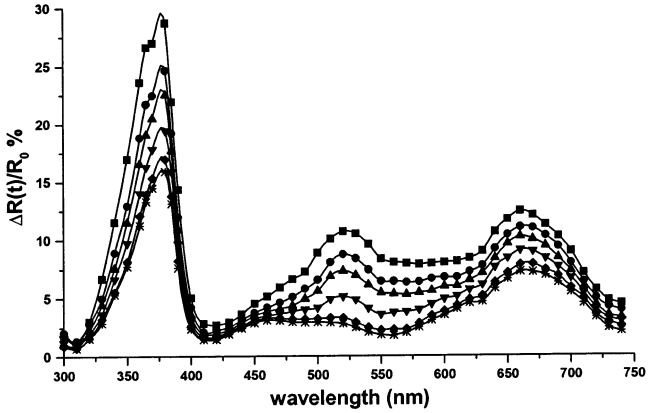

Figure 3. Diffuse reflectance transient UV−visible absorption spectra of photoexcited BP occluded in $Na_{85}FAU$ at 4 BP/UC loading recorded at different delay times 1.5 (■), 5 (●), 10 (▲), 30 (▼), 90 (◆), and 130 (*) μs after laser pump excitation (248 nm, 10 ns, 1.5 mJ·cm^{-2}).

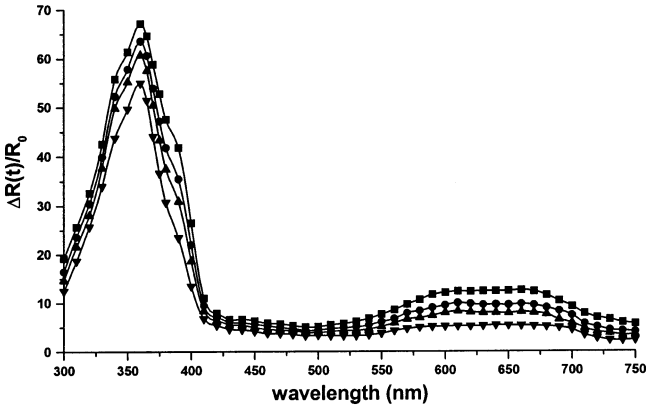

Figure 4. Diffuse reflectance transient UV−visible absorption spectra of photoexcited BP occluded in $Na_{85}FAU$ at 8 BP/UC loading recorded at different delay times 1.5 (■), 5 (●), 10 (▲), and 30 (▼) μs after laser pump excitation (248 nm, 10 ns, 1.5 mJ·cm^{-2}).

coupled with the observation of $BP^{\bullet+}$. However, it should be noted that the shape of the absorption band around 510 nm changes significantly during the decays of the transient species and suggests more than one electron trapping site. The extracted spectrum of $BP^{\bullet+}$, Figure 5b, exhibits supplementary features with a maximum around 460 nm. These features cannot be assigned to any electronic transition of $BP^{\bullet+}$ but were attributed to the remaining absorption of trapped electrons not resolved by the SIMPLISMA approach. This finding suggests simultaneous $BP^{\bullet+}$ and trapped electron decays after disappearance of the Na_4^{3+} cluster. At a lower laser fluence, the major transient species was found to be $BP(T_1)$ through a monophotonic process, and at higher laser fluence the photoionization was found to be predominant through a biphotonic process.[6] The photolysis of bare Na_nX with our experimental conditions (248 nm, 0.2−4 mJ) does not lead to transient absorption around 500 nm. In the present work, the trapped electrons are generated exclusively by photoionization of occluded BP, as previously observed for other electron donor polyaromatics.

The increase of loading values to 2 and 4 BP/UC gives rise to a more intense band around 510 nm, Figure 3. SIMPLISMA analysis of spectra sets permits us to extract three spectra straightforwardly attributed to $BP(T_1)$, $BP^{\bullet+}$, and the Na_4^{3+} cluster, Figure 5a,b,d. At a lower laser fluence, the major transient species was found to be $BP(T_1)$, and at a higher laser fluence the photoionization was found to be predominant.

Aliquots of water corresponding to 32 H_2O/UC loading were introduced to the 2 BP/UC zeolite sample to check the effect

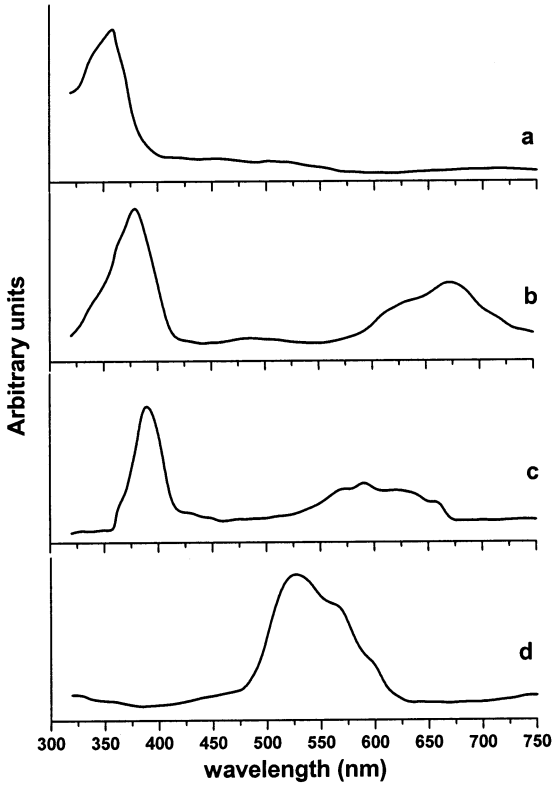

Figure 5. UV−visible absorption spectra of transient species occluded in Na_nFAU ($n = 85, 96$) generated by laser photolysis: (a) BP in triplet state $BP(T_1)$; (b) BP radical cation $BP^{\bullet+}$; (c) BP radical anion $BP^{\bullet-}$; (d) Na_4^{3+}. The spectra were extracted by data processing of the overall spectral data.

of possible residual water on the photochemical behavior of occluded BP. After an equilibrium period of 1 month the transient absorption spectra were recorded. The DRTUV spectra were found to be typical of $BP^{\bullet+}$ and $BP(T_1)$ species; however the absorption of Na_4^{3+} at 510 nm decreases dramatically upon addition of water. This finding is in agreement with previous work related to the photochemical study of BP occluded at low loading in hydrated NaY ($Na_{51}FAU$) faujasitic zeolite and naphthalene occluded in NaX.[6]

At 8 BP/UC loading the feature at 530 nm was not observed in the transient spectra. In contrast, shoulders are apparent at 400 and 600 nm, Figure 4. SIMPLISMA analysis of the data sets permits us to extract three spectra over the experimental time range. Two spectra were straightforwardly attributed to $BP(T_1)$ and $BP^{\bullet+}$, Figure 5a,b. The third spectrum, Figure 5d, contains two bands at 395 and 600 nm assigned to $*BP^{\bullet-} \leftarrow BP^{\bullet-}$ transitions by comparison with spectra obtained in solution.[2] At high loading, the radical anion can be formed by intercepting photoejected electron. In the experimental time scale the formation of $BP^{\bullet-}$ appears coupled with the observation of $BP^{\bullet+}$ and the capture of photoejected electron as Na_4^{3+} is found to be negligible. An analogous trend was observed previously during the photolysis of BP occluded at high loading in hydrated NaY.[6]

Time-Resolved Resonance Raman (TR^3) Scattering. A 248 nm pump wavelength was used to generate the transient species. Nevertheless, the TR^3 experimental setup requires us to focus the laser beam on a small spot of the sample. So, the lower laser fluence used was 4 mJ·cm^{-2} and corresponds to the higher value used for transient absorption experiments. The UV absorption bands of $BP(T_1)$, $BP^{\bullet+}$, and $BP^{\bullet-}$ overlap in the same wavelength region, 360, 375, and 395 nm, respectively, whereas

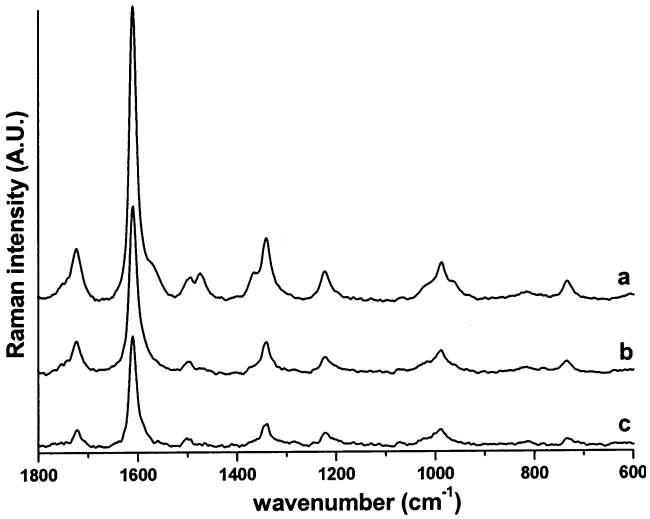

Figure 6. Time-resolved resonance Raman spectra of photoexcited BP occluded in $Na_{85}FAU$ at 1 BP/UC loading probed at 370 nm (8 ns, 4 mJ·cm^{-2}) and recorded at different delay times after laser pump excitation (248 nm, 10 ns, 6 mJ·cm^{-2}): (a) 50 ns; (b) 1 μs; (c) 10 μs.

$BP^{\bullet+}$ and $BP^{\bullet-}$ exhibit visible absorption bands at 650 and 600 nm with weaker absorption coefficients. RR scattering was excited using the 370 nm probe wavelength, and spectra were recorded between 1800 and 600 cm^{-1}. So far, attempts to record TR^3 spectra probed at 625 nm failed. The delay times between pump and probe pulses were in the 50 ns to 100 μs range. Spectra acquired with only 370 nm probe pulses without any pump pulse showed exclusively the Raman features of occluded $BP(S_0)$ and zeolite.

TR^3 spectra of photoexcited BP occluded (1 BP/UC) in Na_{85}-FAU are shown in Figure 6, after the subtraction of weak off-resonant Raman features of $BP(S_0)$. This Figure 6 is typical of the TR^3 results obtained with occluded BP with 1, 2, and 4 BP/UC loading values in Na_nFAU (n = 85, 96). Two distinct species with different lifetimes were observed. With a 50 ns delay time, prominent resonance Raman bands of $BP^{\bullet+}$ were observed at 1724, 1615, 1502, 1342, 1224, 1018, 989, and 737 cm^{-1} with some minor bands and shoulders observed at 1570, 1476, 1366, and 964 cm^{-1}. With delay times higher than 1 μs, only the $BP^{\bullet+}$ spectrum was detected, Figure 6b,c. Difference spectra between spectra recorded at 50 ns and 1 μs delay times indicate more clearly the $BP(T_1)$ characteristics, Figure 8c.[2] Analogous TR^3 behavior was previously observed for photoexcited BP in acetonitrile solution. The four minor bands at 1570, 1476, 1366, and 964 cm^{-1} correspond to the most prominent TR^3 features exhibited by $BP(T_1)$ in cyclohexane solution under 370 nm excitation.[2] The wavenumbers and the relative intensities of the Raman features of $BP(T_1)$ and $BP^{\bullet+}$ were found to be analogous in solution and in the void space of Na_nFAU zeolites, respectively.[7] These spectroscopic analogies suggest structural analogies between the transient species in solution and in the void space of Na_nFAU zeolites. The assignment of the RR bands of these transient species to nearly planar structures in solution were previously performed.[2] As expected from previous theoretical calculations, $BP(T_1)$ exhibits planar quinone-like structure and $BP^{\bullet+}$ is found to be nearly planar with quinoidal structure.[3,30]

TR^3 spectra of photoexcited BP occluded (8 BP/UC) in Na_{85}-FAU are shown in Figure 7 after subtraction of the Raman features of the $BP(S_0)$. This Figure 7 is typical of the TR^3 results obtained with occluded BP at high loading values in Na_nFAU (n = 85, 96). With a 50 ns delay time, the most prominent RR bands of $BP^{\bullet+}$ were observed with many supplementary bands.

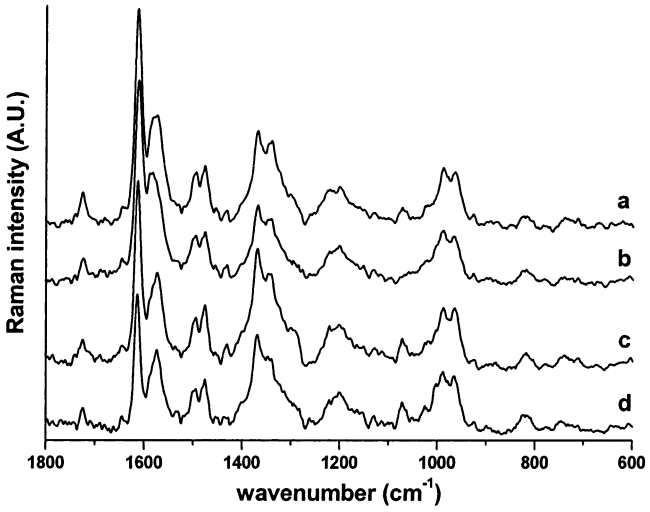

Figure 7. Time-resolved resonance Raman spectra of photoexcited BP occluded in $Na_{85}FAU$ at 8 BP/UC loading probed at 370 nm (8 ns, 4 mJ·cm^{-2}) and recorded at different delay times after laser pump excitation (248 nm, 10 ns, 6 mJ·cm^{-2}): (a) 50 ns; (b) 1 μs; (c) 10 μs; (d) 90 μs.

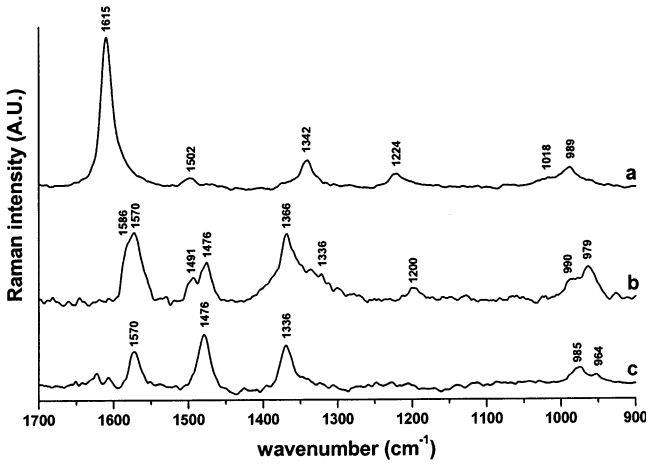

Figure 8. Resonance Raman scattering spectra of transient species occluded in Na_nFAU (n = 85, 96) generated by laser photolysis and excited at 370 nm: (a) BP radical cation $BP^{\bullet+}$; (b) BP radical anion $BP^{\bullet-}$ and BP in triplet state $BP(T_1)$; (c) BP in triplet state $BP(T_1)$. The spectra were obtained by difference of experimental spectra.

For 1, 10, and 90 μs delay times, analogous TR^3 spectra were detected. After subtraction from the spectra of the RR contribution of $BP^{\bullet+}$, the 1570, 1476, 1366, 985, and 964 cm^{-1} supplementary bands were straightforwardly attributed to $BP(T_1)$ whereas the remaining bands and shoulders at 1586, 1491, 1326, 1200, 990, and 979 cm^{-1} were found to be in agreement with the vibrational modes of $BP^{\bullet-}$ with a nearly planar quinone-like structure, Figure 8b.[1,31] Three distinct species $BP(T_1)$, $BP^{\bullet+}$, and $BP^{\bullet-}$ were simultaneously observed in the 50 ns to 100 μs experimental time range. Analogous TR^3 behavior was observed for photoexcited BP in alcohol solution.[1]

Kinetics. Figure 9 exhibits specific concentration decays of $BP(T_1)$, $BP^{\bullet+}$, Na_4^{3+}, and $BP^{\bullet-}$ obtained by SIMPLISMA analysis of DRTUV data set of the 4 BP/UC sample.

This Figure 9 is typical of all $BP(T_1)$, $BP^{\bullet+}$, and Na_4^{3+} concentration decays obtained with 1, 2, and 4 BP/UC loading values in Na_nFAU (n = 85, 96) between 1 and 340 μs. The decays were simulated according to several kinetic models detailed in the Experimental Section. However, only the Albery function provides an adequate description of the experimental decays, Figure 9.

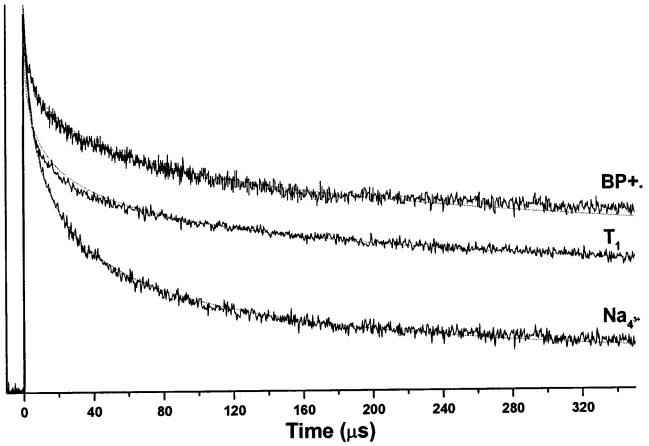

Figure 9. Decay profiles of concentration of transient species occluded in $Na_{85}FAU$ at 4 BP/UC loading generated by laser photolysis: BP radical cation $BP^{\bullet+}$; BP in triplet state $BP(T_1)$; Na_4^{3+}. The concentration values were extracted by data processing of the experimental absorption decays. The solid lines represent the best calculated decays using the Albery function (see Experimental Section).

TABLE 1: Average First-Order Rate Constant $\bar{k}$ (s^{-1}) and Corresponding Distribution Coefficient γ, In Parentheses, of the Decays of the Transient Species Generated by Fast Laser Photolysis of Biphenyl (BP) Occluded in X Faujasitic Zeolites

BP/unit cell	$\bar{k}$ $BP(T_1)$	$\bar{k}$ $BP^{\bullet+}$	$\bar{k}$ Na_4^{3+}	$\bar{k}$ $BP^{\bullet-}$
1 BP/$Na_{85}FAU$	15×10^3 (3)	1.8×10^3 (3)	70×10^3 (3)	
2 BP/$Na_{85}FAU$	20×10^3 (3)	2.0×10^3 (3)	140×10^3 (3)	
2 BP/$Na_{96}FAU$	25×10^3 (4)	2.2×10^3 (4)	10×10^3 (4)	
4 BP/$Na_{85}FAU$	25×10^3 (5)	3.6×10^3 (5)	400×10^3 (5)	
8 BP/$Na_{85}FAU$	$\sim 9 \times 10^3$ (5)	80×10^3 (5)		50×10^3 (5)

This Gaussian distribution kinetic model, which was developed by Albery, is based on a dispersion of first-order rate constants $k = \bar{k} \exp(\gamma x)$, where $\bar{k}$ is the average rate constant and γ is the width of the distribution. According to the model, concentration decays can be represented by

$$C(t) = C/C_0 = \int_{+\infty}^{-\infty} \exp(-x^2) \exp(-\bar{k}t \exp(\gamma X))\, dx / \int_{+\infty}^{-\infty} \exp(-x^2)\, dx \quad (6)$$

where $\int_{-\infty}^{+\infty} \exp(-x^2)\, dx = \sqrt{\pi}$ and $C(t)$ is the normalized concentration.

If $\gamma = 0$ (no dispersion), eq 6 is reduced to first-order kinetics: $C(t) = \exp(-kt)$. A simple numerical procedure for integrating the numerator in eq 6 using only $\bar{k}$ and γ parameters was detailed in appendix of the original publication.[22] The Albery function has already been used for the description of the decay kinetics of several transient species in zeolites as well as in other heterogeneous media.[23,32,33] The adequacy of this function for a significant part of decay kinetics of $BP(T_1)$, $BP^{\bullet+}$, Na_4^{3+}, and $BP^{\bullet-}$ indicates the heterogeneous behavior of kinetics. The best values of $\bar{k}$ average rate constants deduced by fitting are listed in Table 1. The corresponding γ distribution coefficients were found to be between 3 and 5 and are in reasonable agreement with other heterogeneous photochemical reactions. The corresponding mean lifetimes are conventionally represented by $1/\bar{k}$.

T_1 population and ionization are two parallel photolytic processes that arise concurrently in the void space of X zeolites. UV photolysis at low laser fluence value generates $BP(T_1)$ as the major species, whereas photolysis at high fluence value generates both $BP(T_1)$ and ionization.

Decay of the BP(T_1) Triplet State. The $BP(T_1)$ mean lifetime values appear independent of the ionization yield. The $BP(T_1)$ lifetime value was found to be around 50 μs below 4 BP/UC loading, Table 1. In contrast, above 4 BP/UC the estimated mean lifetime of $BP(T_1)$ increases dramatically to reach approximately 110 μs for 8 BP/UC loading, Table 1. Assumption of a Gaussian distribution demonstrates effectively the heterogeneity of the annihilation of the triplet state, which is found to be slower at higher loading. A non-Gaussian lifetime distribution analysis was not undertaken.[34] The presence of numerous BP molecules in the porous void at high loading hinders the mobility and probably shields $BP(T_1)$ from energy transfer. Direct triplet−triplet annihilation, which requires an encounter between two $BP(T_1)$, can occur but is expected to be very fast and scarce. However, according to the relatively long lifetime values, it is more reasonable to postulate a triplet energy transfer mechanism by energy acceptors such as zeolite framework and $BP(S_0)$.[35]

Decays of $BP^{\bullet+}$, Na_4^{3+}, and $BP^{\bullet-}$. Photoionization to produce $BP^{\bullet+}$ and a photoejected electron is dominant at high pump laser fluence. The $BP^{\bullet+}$ mean lifetime value was estimated to be around 500 μs at 1 BP/UC and weakly depend on the loading value below 4 BP/UC, Table 1. The mean lifetime of the Na_4^{3+} cluster is found to be dramatically shorter than that for $BP^{\bullet+}$ (20 μs for 4 BP/UC) and is found to depend markedly on the number of Na^+ extraframework cations of the zeolite, Table 1. The Na_4^{3+} cluster yield increases dramatically from 1 BP to 4 BP/UC loading and is practically zero at 8 BP/UC loading. It should be noted that Na_4^{3+} is not the exclusive electron trapping site, because after the decay of Na_4^{3+} the remaining electronic absorptions appear around 460 nm, assumed to be typical of supplementary zeolite capturing electron sites. The SIMPLISMA approach does not resolve these 460 nm absorptions, which appear to decrease simultaneously with $BP^{\bullet+}$ absorptions. It is clear that electron recapturing by $BP^{\bullet+}$ implies electron-transferability of extraframework cations and zeolite framework.

The $BP^{\bullet+}$ mean lifetime decreases dramatically above 4 BP/UC loading and was found to be approximately 12 μs for 8 BP/UC loading, whereas the $BP^{\bullet-}$ mean lifetime is found to be significantly higher, 20 μs. $BP^{\bullet-}$ is formed by direct capture of a photoejected electron by electron scavenger $BP(S_0)$ before any interception by Na^+ cations. The geminate $BP^{\bullet+}-BP^{\bullet-}$ recombination can occur, but it is more probable that the recombination occurs via an electron-transfer process with the zeolite framework.

Discussion

Photophysical and photochemical properties of BP occluded in zeolites were found to be highly dependent on the loading value. The loading level has a dramatic effect on sorption sites and dynamics of $BP(S_0)$ within the porous void space. Previous work provides structural, energetic, and dynamic behaviors of $BP(S_0)$ in Na_nFAU as a function of BP loading.[14] The most significant results for the present study are briefly summarized below.

Before excitation, biphenyl is occluded as $BP(S_0)$ intact molecules in Na_nFAU zeolites. At low loading corresponding to 1 BP per unit cell or 1 BP per 8 supercages, the BP molecule lies preferentially in the supercage in a twisted conformation with each phenyl group facially coordinated to extraframework Na^+, Figure 1A. An occupancy of 2 BP per supercage is significant only at 8 BP/UC or 1 BP per supercage average loading, Figure 1B. However, BP occupancy of supercages is not uniform, some supercages contain 2 BP, some contain 1 BP, and the remaining are empty. The occupancy of the void space is not static, and a recent molecular dynamics study indicates the main trends of BP dynamic behavior within the

porous void. At low loading, BP carries out rotational, translational, and torsional motions between several sorption sites inside one supercage and can jump several times to other supercages over 1 ns simulation time at room temperature. The BP molecule and Na^+ cation dynamic behaviors are highly correlated. The BP diffusion is markedly reduced at high loading by 2 BP occupancy per supercage. The BP molecule and Na^+ cation dynamic behaviors are highly correlated.[14] During the laser pulse (10 ns) BP can jump many times to different supercages at low loadings, but this mobility is markedly reduced at high loading.

As expected from photolysis studies in solution, the lifetime of $BP(S_1)$ is less than 50 ns in the void space of X zeolites and was not observed in the present work. Probably, the photoexcited S_3 state relaxes rapidly to the S_1 state, then $BP(S_1)$ generates $BP(T_1)$ through intersystem conversion. The structure of the occluded $BP(T_1)$ was found to be analogous to the quinoidal structure exhibited in solution. During decay, $BP(T_1)$ can occupy probably several supercages and a triplet annihilation mechanism occurs probably through energy transfer with zeolite framework and $BP(S_0)$, as reported previously in other energy transfer studies in zeolites.[35] The increase of the $BP(T_1)$ lifetime with increasing loading level is in complete disagreement with the triplet lifetime decrease of anthracene with increasing loading level in NaY zeolite.[36] This latter finding was ascribed to triplet quenching by anthracene in the ground state. In our case 2 BP occupancy per supercage at high loading should promote such behavior for occluded BP. Nevertheless, low molecular mobility and ionization can hinder $BP(T_1)$ quenching at high loading.

One photon direct ionization of occluded $BP(S_0)$ is unlikely and $BP^{\bullet+}$ is considered to take place by a biphotonic process, as previously reported in Na_{51}FAU zeolite.[6] The high electrostatic field within the porous void can explain the higher ionization yield of occluded BP with respect to ionization yield in acetonitrile solution. The structure of occluded $BP^{\bullet+}$ is found to be planar, as previously reported in solution.[2]

At low loading, the photoejected electron is primarily trapped as a Na_4^{3+} cluster, and the electron transfer from Na_4^{3+} to another trapping site occurs faster than to $BP^{\bullet+}$ before recombination. The $BP^{\bullet+}$ mean lifetime was found to be significantly longer in Na_{85}FAU at low loading than in acetonitrile solution.[2] Acetonitrile is known to solvate tightly with an electron in the form of the acetonitrile anion aggregate. It is reasonable to propose the following mechanism of laser ionization of BP occluded at low loading (1, 2, 4 BP/UC) in Na_nFAU ($n = 85$, 96).

$$BP/Na_n(AlO_2)_n(SiO_2)_{192-n} + h\nu \rightarrow BP^{\bullet+}/Na_n(AlO_2)_n(SiO_2)_{192-n} + e \quad (7)$$

The photoejected electron e is trapped by the extraframework Na^+ cation to form $Na_n^{(n-1)+}$ clusters:

$$BP^{\bullet+}/Na_n(AlO_2)_n(SiO_2)_{192-n} + e \rightarrow BP^{\bullet+}/Na_n^{(n-1)\bullet+}(AlO_2)_n(SiO_2)_{192-n} \quad (8)$$

The trapped electron migrates from the $Na_n^{(n-1)+}$ cluster to another zeolite site:

$$BP^{\bullet+}/Na_n^{(n-1)\bullet+}(AlO_2)_n(SiO_2)_{192-n} \rightarrow BP^{\bullet+}/Na_n(AlO_2)_n(SiO_2)_{192-n}^{\bullet-} \quad (9)$$

The $BP(S_0)$ ground state is restored through

$$BP^{\bullet+}/Na_n(AlO_2)_n(SiO_2)_{192-n}^{\bullet-} \rightarrow BP/Na_n(AlO_2)_n(SiO_2)_{192-n}^{\bullet-\bullet+} \quad (10)$$

Finally, the trapped electron and positive hole recombine to restore the neutral zeolite.

$$BP/Na_n(AlO_2)_n(SiO_2)_{192-n}^{\bullet-\bullet+} \rightarrow BP/Na_n(AlO_2)_n(SiO_2)_{192-n} \quad (11)$$

At high loading, the photoejected electron is likely trapped by $BP(S_0)$ in close proximity. BP is a typical electron scavenger. The $BP^{\bullet+}$ mean lifetime was found to be markedly shorter than at low loading, whereas the $BP^{\bullet-}$ mean lifetime is found to be somewhat higher than that of $BP^{\bullet+}$. The lifetimes of these radical ions are dramatically longer in the void space of X zeolite than in alcohol solution.[1] The geminate $BP^{\bullet+}-BP^{\bullet-}$ recombination can occur before 50 ns, but it is more probable that the recombination occurs via an electron-transfer process with the zeolite framework.

The large cavity (1.2 nm) faujasitic zeolites exhibit the ability to stabilize radical species generated by photoinduced intermolecular electron-transfer reaction of biphenyl with respect to polar solvents through the trapping of photoejected electron. However, the medium pore (0.55 nm) zeolites such as Al−ZSM-5 hinder more efficiently the back electron transfer and stabilize more efficiently $BP^{\bullet+}$.[8]

Conclusions

The fast laser UV photolysis of biphenyl occluded in dehydrated aluminum rich faujasitic X zeolites generates biphenyl in the triplet state, biphenyl radical cation, trapped electron, and biphenyl radical anion.

The triplet state is generated predominantly at low laser fluence. The molecular structures of occluded BP transient species were found to be planar, as reported in solution. The mean lifetimes of the triplet state are found to be around 100 μs, and the quenching occurs by the energy acceptor zeolite framework and also biphenyl in the ground state.

Photoionization to produce the biphenyl radical cation and photoejected electron is dominant at high pump laser fluence. At low loading, the planar radical cation is produced in high yield. The photoejected electron is trapped primarily as part of an Na_4^{3+} cluster. The recombination process includes several electron transfers with the host. At high loading, the biphenyl anion radical forms as a result of the photoejected electron capture by a biphenyl molecule in the ground state. The large cavity (1.2 nm) faujasitic zeolites exhibit the ability to stabilize the biphenyl radical species generated by photoinduced intermolecular electron-transfer reaction of biphenyl with respect to polar solvents through the trapping of photoejected electrons.

Acknowledgment. The Centre d'Etudes et de Recherches Lasers et Applications (CERLA) is supported by the Ministère chargé de la recherche, the région Nord/Pas de Calais, and the Fonds Européen de Développement Economique des Régions.

References and Notes

(1) Sasaki, Y.; Hamaguchi, H. *J. Chem. Phys.* **1999**, *110*, 9179−9185.
(2) Buntinx, G.; Poizat, O. *J. Chem. Phys.* **1989**, *91*, 2153-2162.
(3) Pan, D.; Shoute, L. C. T.; Phillips, D. L. *Chem. Phys. Lett.* **2000**, *316*, 395−403.
(4) Hashimoto, S.; Thomas, J. K. *Photochem. Photobiol. A: Chem.* **1991**, *55*, 377−386.
(5) Mao, Y.; Thomas, J. K. J. *Chem. Soc. Faraday Trans.* **1992**, *88*, 3079−3086.

(6) Hashimoto, S.; Mutoh, T.; Fukumura, H.; Masuhara, H. *J. Chem. Soc., Faraday Trans*. **1996**, *92*, 3653−3660.
(7) Brémard, C.; Buntinx, G.; De Waele, V.; Didierjean, C.; Gener, I.; Poizat, O. *J. Mol. Struct.* **1999**, *480*−*481*, 69−81.
(8) Gener, I.; Buntinx, G.; Brémard, C. *Angew. Chem., Int. Ed. Engl.* **1999**, *38*, 1819−1822.
(9) Thomas, J. K. *Chem. Rev*. **1993**, *93*, 301−3020.
(10) Yoon, K. B. *Chem. Rev*. **1993**, *93*, 321−339.
(11) Ramamurthy, V.; Lakshminarasimhan, P.; Grey, C. P.; Johnston, L. J. *Chem. Commun*. **1998**, 2411−2424.
(12) Scaiano, J. C.; Garcia, H. *Acc. Chem. Res.* **1999**, *32*, 783−793.
(13) Ramamurthy, V. *J. Photochem. Photobiol. C: Chem. Rev*. **2000**, *1*, 145−166.
(14) Gener, I.; Ginestet, G.; Buntinx, G.; Brémard, C. *Phys. Chem. Chem. Phys*. **2000**, *2*, 1855−1864.
(15) Brémard, C.; Le Maire, M. *J. Phys. Chem.* **1993**, *97*, 9695−9702.
(16) Wilkinson, F.; Willsher, C. J. *Appl. Spectrosc*. **1984**, *38*, 897−901.
(17) Buntinx, G.; Ginestet, G.; Gener, I.; Coustillier, G.; Brémard, C. *Laser Chem.* **1999**, *19*, 325.
(18) Windig, W.; Guilment, J. *Anal. Chem.* **1991**, *63*, 1425−1432.
(19) Windig, W. *Chemom. Intell. Lab. Syst.* **1997**, *36*, 3−16.
(20) Windig, W.; Stephenson, D. A. *Anal. Chem.* **1992**, *64*, 2735−2742.
(21) Windig, W. *Chemom. Intell. Lab. Syst.* **1994**, *23*, 71−86.
(22) Albery, W. J.; Bartlett, P. N.; Wilde, C. P.; Darwent, J. R. *J. Am. Chem. Soc.* **1985**, *107*, 1854−1858.
(23) Levin, P. P.; Ferreira, L. F. V.; Costa, S. M. B. *Langmuir* **1993**, *9*, 1001−1008.
(24) Olson, D. H. *Zeolites* **1995**, *15*, 439−443.
(25) Porcher, F.; Souhassou, M.; Dusausoy, Y.; Lecomte, C. *Eur. J. Mineral*. **1999**, *11*, 333−343.
(26) Cozens, F. L.; Régimbald, M.; Garcia, H.; Scaiano, J. C. *J. Phys. Chem.* **1996**, *100*, 18165−18172.
(27) Liu, X.; Zhang, G.; Thomas, J. K. *J. Phys. Chem.* **1995**, *99*, 10024−10034.
(28) Edwards, P. P.; Anderson, P. A.; Thomas, J. M. *Acc. Chem. Res.* **1996**, *29*, 23−29.
(29) Shibata, W.; Seff, K. *J. Phys. Chem.* **1997**, *101*, 9022−9026.
(30) Lee, S. Y. *Bull. Korean Chem. Soc.* **1998**, *19*, 93−98.
(31) Furuya, K.; Torii, H.; Furukawa, Y.; Tasumi, M. *J. Mol. Struct. (THEOCHEM)* **1998**, *424*, 225−235.
(32) Jonhston, L. J.; Scaiano, J. C.; Shi, J. L.; Siebrand, W.; Zerbetto, F. *J. Phys. Chem.* **1991**, *95*, 10018−10024.
(33) Pankasem, S.; Thomas, J. K. *J. Phys. Chem.* **1991**, *95*, 6990−6996.
(34) Barra, M.; Scaiano, J. C. *Photochem. Photobiol.* **1995**, *62*, 60−65.
(35) Cano, M. L.; Cozens, F. L.; Garcia, H.; Scaiano, J. C. *J. Phys. Chem.* **1996**, *100*, 18152−18157.
(36) Hashimoto, S.; Hagiri, M.; Barzynkin, A. V. *J. Phys. Chem. B* **2002**, *106*, 844−852.